Version of Record: https://www.sciencedirect.com/science/article/pii/S138358662200209X
Manuscript_74bfa0c465544b4ee261c1aa3df090a9

Acoustic Focusing of Microplastics in Microfabricated and Steel Tube Devices: An Experimental Study on the Effects from Particle Size and Medium Density.

Lumala Nelum Perera and Menake E. Piyasena*

Department of Chemistry, New Mexico Institute of Mining and Technology, Socorro, NM 87801

Corresponding Author:

Menake E. Piyasena

sesathpura.piyasena@nmt.edu

+1-575-835-6162

© 2022 published by Elsevier. This manuscript is made available under the Elsevier user license
https://www.elsevier.com/open-access/userlicense/1.0/

Abstract

The contamination of aquatic systems with microplastics is becoming a severe threat to living organisms. Microplastics found in the environment consist of a wide range of particle sizes thus give rise to several challenges to current purification methods. Acoustic focusing has been utilized as a particle concentrating method in biological and non-biological applications. In this study, we investigate the feasibility of using acoustic focusing technology to isolate microplastics in aqueous samples and find that a two-stage mechanism is essential to concentrate microplastics of wide size ranges of the same material. We demonstrate for the first time experimentally that when the particle size is comparable to the resonance wavelength, they deviate from typical pressure nodal focusing and show pressure antinodal focusing. Further, we have expanded microplastics isolation beyond microfluidic systems and demonstrate their extraction capabilities relatively at higher flow rates using microplastics of polystyrene, polyethylene, and polymethyl methacrylate ranging from 6 µm to 300 µm diameter and in devices fabricated with cylindrical steel tubes. We could extract 70% of microplastics smaller than 180 µm and 82% of microplastics greater than 180 µm in diameter from an aqueous sample at a flow rate of 12 mL/min. We demonstrate that small microplastics focus on acoustic pressure nodes regardless of the medium density. However, focusing of large microplastics of the same material depends on the medium density.

Key words – Microplastic, Acoustic focusing, Acoustic steel device, Water purification, Microfluidic

Abbreviations

MPs- Microplastics

PE- Polyethylene

PS- Polystyrene

PVC- Polyvinylchloride

PMMA- Polymethyl methacrylate

PDMS- Polydimethylsiloxane

DMSO- Dimethyl sulfoxide

ARF- Acoustic radiation force

1. Introduction

Microplastics (MPs) are emerging as environmental pollutants and posing a threat to the global marine and freshwater systems at an alarming level [1, 2] and demand immediate mitigation and reduction plans. However, the existing MP removal methods have some inherent limitations that prevent their further improvements. Therefore, the development of rapid and effective MP isolation methods is highly desirable.

Generally, plastics with diameters ranging from 100 nm to 5 mm are considered microplastics [3, 4]. MPs present as constituents of personal care and cleaning products are classified as primary microplastics [5], while MPs derived from degraded plastic debris are classified as secondary microplastics. Microplastic pollution of water bodies is not just limited to populated regions, and recent studies have found microplastic contaminants in remote regions, including the Arctic [6, 7]. Large amounts of secondary MPs are derived from polymers like polyethylene (PE), polystyrene (PS), polypropylene, and polyvinyl chloride (PVC) [8], the major polymer materials found in consumer plastic products like bags, wraps, bottles, and food containers. They are often used as disposable products, thus rapidly accumulate as wastes in nature. Further, secondary MPs resulting from microbial action, road abrasion, UV degradation, and fragmentation of released plastics cause further accumulation of a vast amount of MPs in the environment [9]. Even biodegradable plastics has been found to generate a significant amount of secondary MPs [10]. In addition to these sources, laundry effluent adds significant microplastic waste to nature [11, 12].

Geyer et al. estimated that 8.3 billion metric tons of virgin plastics have been produced to date. If the current production and waste management methods continue, roughly 12,000 metric tons of plastic waste will be anticipated in the natural environment by 2050 [13]. MPs accumulated in oceans act as a source of greenhouse gases [14]. Besides, they adsorb other pollutants like heavy metals, PCB, and DDT [15]. Furthermore, the ingestion of MPs by fish [16, 17] and other

aquatic species [18, 19] poses a risk to human health by consuming aquatic food sources [20]. Further, the consumption of water contaminated with MPs [21] results in releasing toxic constituents and adsorbed pollutants to the body. Considering these undesirable impacts of MPs, minimizing their release to the natural and human-made water systems is essential.

Currently, MPs are removed mainly by filtering, elutriation, and density separation [22-24]. They are subjected to clogging; thus, frequent cleaning and replacement of membranes or filters are necessary. Furthermore, these methods are time consuming and less beneficial for the simultaneous removal of MPs of different sizes and types present in the environment. For example, the sieve size determines the smallest size of MPs that can be removed via filters. Since different MP types have different densities, elutriation and density separation will not be competent for all MPs. Besides, other removal methods like nets and bags [4] are less effective due to the necessity of extensive labor. Therefore finding more effective, efficient, and real-time MP removal methods are essential.

Recently Chen *et al.* demonstrated the concentrating of MPs using inertial focusing in microfluidic devices [25]. They have demonstrated removal of MPs up to 50 µm in diameter at a maximum flow rate of 2.1 mL/min. Acoustic focusing has also been used to concentrate and isolate particulate matter suspended in fluid and real-time. The interaction of resonance standing acoustic waves with particles significantly smaller than the wavelength and suspended in a fluid generates primary acoustic radiation forces (F_{rad}) that move particles to specific regions of a resonating acoustic chamber. The acoustic radiation force on a particle that is much smaller than the wavelength is given by equation (1)[26, 27].

$$F_{rad} = -\frac{\pi p_0^2 V_P \beta_m}{2\lambda} \phi(\beta, \rho)\, sin\, 2kx \qquad (1)$$

$$\phi(\beta, \rho) = \frac{5\rho_p - 2\rho_m}{2\rho_p + \rho_m} - \frac{\beta_p}{\beta_m} \quad (2)$$

Where p, V, β, ρ, k, λ, and x refer to the pressure amplitude of the standing wave, the volume of the particle, compressibility, density, wave number, wavelength, and distance to the particle from the pressure node, respectively. Subscripts, p and m, represent the particle and the medium, respectively. It suggests that acoustic radiation forces increase with the cubed radii of the particle. The acoustic contrast factor (ϕ) shown in equation (2) depends on the difference in the density and the compressibility of particles to the suspended medium. It determines the transverse positioning of particles in a resonating chamber. Particles with a positive contrast factor will move to the pressure nodes, while particles with a negative contrast factor will move to the pressure anti-nodes of the standing acoustic waves [26]. However, equation 1 is only accurate for particles that are much smaller than the wavelength of the applied frequency. Inter-particle scattering acting on a particle is resulted from an acoustic wave scattered off from another particle. When the inter-particle distance is larger than the diameter of two particles, and the wavelength is larger than particle diameters, the inter-particle scattering and hence the secondary radiation forces on the small particles are negligible [28]. However, when the particle diameter is comparable to the wavelength, the interparticle scattering of the acoustic wave is non-negligible, which is ignored in equation (1). Therefore, these large particles will have different transverse positioning in the sound wave compared to small particles of the same material described theoretically by Habibi *et al.* recently [29]. This phenomenon cannot be neglected, especially when handling MPs present in environmental samples, due to their wide size distribution.

Y. Akiyama has recently shown that PS microparticles, polyethylene terephthalate fibers, and Nylon 6 fibers with diameters up to 15 µm can be concentrated to the pressure node of the standing wave located in the middle of a microfluidic resonating chamber [30]. In their work, the assumption was that MPs suspended in water, including wastewater from laundry outlets, regardless of the size and type, yet with similar physical properties such as density and

compressibility would behave similarly in an acoustic field. Hence, particles will be focused to the center of a resonating chamber and can be isolated through the central outlet of a trifurcated microfluidic device via acoustic focusing. This assumption can be erroneous if large microplastics are present. Thus, it is crucial to find the behavior of mixtures of microplastics with a wide size range in an applied acoustic field. In this work, we explore acoustic focusing for the isolation of highly abundant MPs in nature, PS, polymethyl methacrylate (PMMA), and PE in aqueous media with different densities. The range of microplastic used in our study is from 6 µm to 300 µm; this covers the majority of sizes abundant in the environment. In the previous study by Y. Akiyama, the separation of MPs was limited to silicon microfluidic devices, with a maximum flow rate of 150 µL/min. The current study expands to explore the acoustic focusing of larger particles in aqueous media with different densities and in steel tubes at higher flow rates. Steel exhibits good acoustic properties such as high acoustic impedance, density, sound speed, and high quality factor (Q-value), essential attributes for better acoustic focusing devices [31]. The fabrication of steel devices is cost effective, less time consuming, and convenient compared to microfabricated devices. In this study, we report the experimental data for size dependent separation of MPs of the same material using bulk acoustic waves in a flow through format for the first time. The combined effect of high density medium and high particle size/wavelength of the applied frequency is also reported for the first time. Considering the real applications, our findings are critical and essential to designing acoustic focusing devices for a broader range of particle sizes suspended in aqueous media with different densities.

2. Material and Methods

Silicon wafers were purchased from University Wafer Inc. (South Boston, MA). The positive type photoresist (AZ 9260) and its developer were purchased from AZ Electronic Materials (Branchburg, NJ), Borosilicate glass slides were purchased from Applied Microarray Inc. (Tempe, AZ), PE, PMMA, and PS MPs were bought from Cospheric (Santa Barbara, CA). 100%

Contrad® 70 was purchased from Decon Labs Inc. (King of Prussia, PA). Piezoelectric transducers (300 mm x 5 mm) were brought from APC International LTD (Mackeyville, PA), and the steel tubes with varying internal diameters (I.D.) were brought from Amazon. Plastic connecting tubings for the steel tubes were brought from Cole-Parmer (Vernon Hills, IL), Nile Red dye from Thermo Fisher Scientific (Carlsbad, CA). Commercial liquid detergents and commercial fabric softeners.

2.1 Fabrication of acoustic focusing devices

We investigated two flow-through systems to explore the feasibility of using acoustic focusing technology for the isolation and separation of MPs in aqueous samples. First, we characterized acoustic focusing parameters using a microfabricated flow device at low flow rates. Then we constructed a relatively large flow device using steel tubes and explored its performance at higher flow rates.

2.1.1 Construction of microfluidic devices

Two microfluidic devices with the width, height, and length of 486 µm × 312 µm × 4 cm (486 µm device) and 1078-µm × 482 µm × 4 cm (1078-µm device) with trifurcated inlet and outlet were constructed using silicon substrates as reported elsewhere [32](Fig.1 a). Briefly, the microfluidic channel design was photo-patterned on a 100 mm silicon wafer with AZ 9260 positive type photoresist and etched using deep reactive ion etching. The channel dimensions were measured using a profilometer (Zygo ZeGage™). A borosilicate glass slide with pre-drilled holes for inlets and outlets was anodically bonded onto the etched wafer, and silicone tubing were attached for liquid connection. A piezoelectric transducer with a resonance frequency of 2.91 MHz was glued to the surface underneath the channel in the longitudinal direction using epoxy super glue (inset, Fig.1 a). The assembled device was mounted on PDMS slabs adhered to a glass slide. The channels were pre-treated with 100% Contrad® 70 solution for 15 min before

introducing samples via a syringe pump (KdScientific, LEGATO 110) to minimize surface adhesion of MPs.

2.1.2 Construction of steel tube devices

Several acoustic focusing devices were constructed with steel tubes with varying I.D.s, from 1.4 mm to 10 mm. Two 6-cm long identical steel tubes were connected using a 1-cm long transparent silicone tubing in each device. Two 1.58 MHz transducers were attached to the external wall of each steel tube using superglue. The setup was mounted on two PDMS slabs adhered to a glass slide, as shown in Fig. 1 b. A silicone tubing was attached to one of the ends of the steel tube as the inlet, while multiple silicone tubing were connected via a glass holder to the other end of the steel tube as a branched outlet, as shown in Fig.1 b.

2.2 Preparation of microplastic samples

Samples containing PE MPs with the diameters of 6, 10-11, 50, and 150 µm, PS MPs with the diameters of 11, 38-48, and 85-105 µm, and PMMA MPs with the diameters of 5-20, 45-53, and 90-106 µm were prepared with a final concentration of 300 µg/mL in D.I. water. Additionally, aqueous samples composed of PE MPs with diameters of 150, 180-212, and 250-300 µm, and PMMA MPs with a diameter of 200 µm were prepared with the final concentration of 900 µg/mL. To study the influence from detergents in water, MPs were suspended in aqueous media composed of either 1% detergent or 1% detergent plus 1% fabric softener. The concentrations were determined via two methods of particle counting, as described later. The PE and PS particles were fluorescent and thus used as received, while PMMA particles were made fluorescent by soaking them in 0.025 M Nile red dye in DMSO for 3 hours and then rinsing them with DMSO and D. I. water, respectively.

2.3 Acoustic focusing of microplastics in microfluidic devices

Aqueous samples of each MP type were introduced to the respective microfluidic device from the middle inlet while keeping the two lateral inlets closed, using a syringe pump (KD Scientific, LEGATO 110). The acoustically focused MPs were obtained from the trifurcated channel's central outlet and purified water from the two lateral outlets. A small rare earth magnet was kept in the syringe, and an external magnet was used to agitate MPs to keep the sample homogeneously mixed while it was introduced to the device. The resonance acoustic waves were generated using a waveform generator (RIGOL DG1022) and amplified via an RF amplifier (Electronic and innovation 240L). The acoustic parameters (amplitude, applied voltage, and frequency) were monitored via an oscilloscope (Tektronix, TBS 1052b-edu). The focusing of MPs up to 106 µm was investigated using the 486 µm device while the particles larger than 106 µm were investigated using the 1078-µm device. Acoustic focusing of each particle size and type was investigated at varying flow rates from 50 to 800 µL/min, and the optimum voltage for each flow rate was recorded. Next, a mixture of MPs containing all three types up to 106 µm was flowed through the 486 µm device at a maximum flow rate and applied voltage of 800 µL/min and 6.1 V, respectively.

2.4 Acoustic focusing of MPs in steel tube devices

Steel tube devices were rinsed with D.I. water and 100% Contrad® 70, respectively, before the sample introduction. Acoustic wave integration and sample introduction were similar as in microfluidic device experiments. However, the steel tube device had a single inlet and multiple outlets. Focusing of each MP type and size was first monitored at 800 µL/min in 1.4 and 3 mm I.D. tubes and at 8 mL/min in tubes with I.D.s from 4 to 10 mm through the transparent silicone tube connector (Fig. 1 b), while the frequency was tuned from 1.0 MHz to 180 KHz at a maximum applied voltage of 8 V. After the optimum frequency was established, a voltage scan was performed to obtain the lowest possible applied voltage required for the optimum focusing at this flow rate. Once those parameters were obtained, the flow rate was gradually increased to

explore the feasibility of having higher flow rates, and the applied voltage was also gradually increased as needed. A small rare earth magnet and an external magnet were used all the time as in microfluidic experiments to maintain a homogenous mixture.

2.5 Determination of focusing and concentrating efficiency

Once the voltage is optimized for each MP size and type at a given flow rate, acoustic focusing and concentrating efficiency were determined by collecting samples from the central and the two lateral streams of the microfluidic device and comparing the MP concentration in both focused and unfocused conditions. Each measurement was performed at least in triplicates. The concentrations of MPs up to 85-106 µm were measured using an automated cell counter (Countess II, Thermo Fisher Scientific), while the concentrations of MPs larger than 106 µm were measured manually using a custom made cell counting grid with a known volume. For the steel tube devices, the focusing and concentration efficiencies were determined by collecting samples from the branched outlets at the observed optimum voltage and frequency, and flow rate of 12 mL/min.

3. Results and Discussion

3.1 Fabrication of acoustic focusing devices

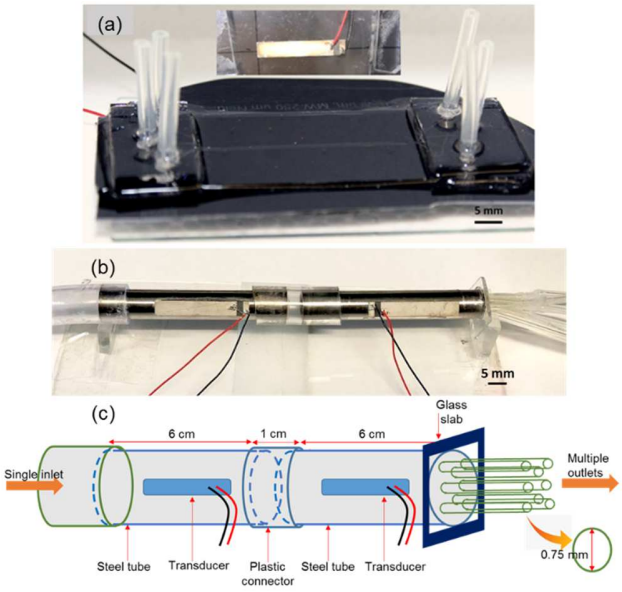

Fig. 1 Acoustic focusing devices constructed with silicon substrates and steel tubes. (a). Silicon acoustofluidic device, the main channel has a dimension of either 486 µm ×312 µm ×4 cm or 1078-µm ×488 µm ×4 cm (width, height, and length, respectively). The channel is enclosed with an anodically bonded Pyrex™ glass slide. The silicone tubing inserted into PDMS slabs are adhered to the glass via plasma bonding and serve as fluidic connectors. The transducer is glued to the backside of the device (inset). (b). Steel acoustofluidic device, the I.D. of the steel tube is 8 mm. Two steel tubes are connected in-line via a transparent plastic tube and two transducers are glued to the side walls. (c). A schematic representation of steel acoustic device (not to the scale).

The two micro-fabricated devices with the width of 486 µm and 1078-µm were used to analyze small and large microplastics, respectively. The experimentally found resonance frequency of the 486-µm device for single node is 1.58 MHz, close to the calculated resonance frequency of 1.52 MHz. The concentrated particles are collected from the middle outlet, while MP-free water is collected from two lateral outlets of the device. Since larger particles can clog this device, we use the 1078-µm device to investigate the focusing of larger MPs (>106 µm). The frequency tuning experiments indicate that this device generates a single pressure node at the optimum

resonance frequency of 710 KHz and the calculated resonance frequency for a single node is 698 KHz. The transducer used to generate this frequency (710 KHz) was most effective at 1.58 MHz, therefore the transducer was not performing at its optimum conditions. This lead to obtaining less focusing and concentrating efficiencies than using optimized transducers. The purpose of having a transparent plastic tube in steel tube devices is to provide an optical window to collect images and videos to determine the extent of particle focusing. Any acoustic damping from the plastic connector was minimized by keeping the plastic tube short and using two resonating steel tubes in-line. Hence, we assumed, there was no change in particle focusing while flowing through the plastic tube.

3.2 Focusing of microplastic in acoustofluidic devices

We investigated acoustic focusing of three types of particles in this study, representing highly abundant MP-pollutants found in the environment [8, 9, 33, 34]. We used three different concentrations of each MP type initially, and we found no concentration effect on the required focusing voltage or the concentrating efficiency; thus, we limited our studies to the following concentrations; 300 µg/mL of small MPs up to 106 µm, and 900 µg/mL of large MPs from 150 µm to 300 µm. We selected these two different concentrations relative to the particle size to maintain a comparable particle count in each sample, hence a similar event rate. The epi-fluorescence microscopic images from the two microfabricated devices (Fig. 2) show the focusing of MP mixtures in the presence of an acoustic field. We observed MPs of 10 to 106 µm in diameter focused on the single pressure node of the 486-µm device regardless of the density of the suspended medium or applied frequency (Fig. 2 b). MPs of 180-300 µm focused on the pressure nodes when the medium was water (Fig. 2 d). However, they focused on the two

pressure anti-nodes of the 1078-µm device when the medium contained 1% (v/v) household detergent and 1% (v/v) fabric softener (Fig. 2 f). The dashed-yellow lines in Fig. 2 c-h indicate the location of pressure nodes, and these images clearly demonstrate the antinodal focusing of larger microplastics. These images were captured near the transducer while the sample is flowing to the right at a flow rate of 500 µL/min. and discrepancies in shapes and sizes of particles are due to the un-even image focusing because of the fast movement of particles in different planes of the device along the z-axis. We made another interesting observation for larger MPs, they aggregated into small chains while being focused onto anti-nodes (Fig. 2 f & h).

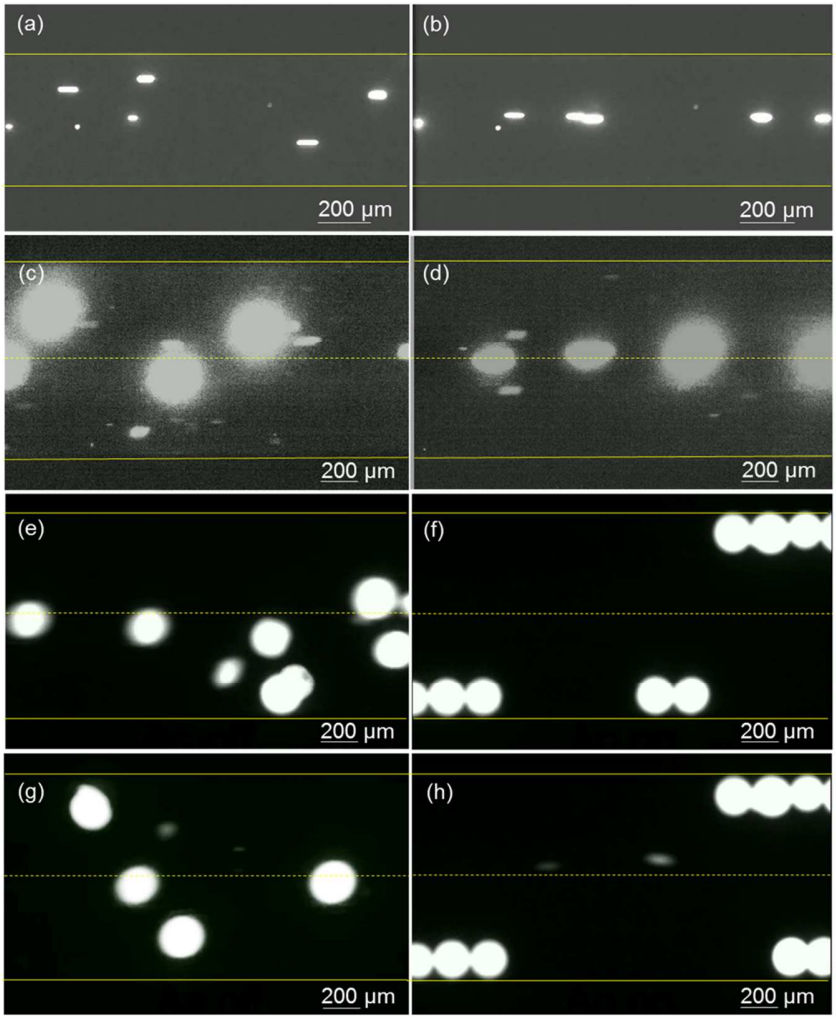

Fig. 2 Epi-fluorescence microscopic images of mixtures of MPs in the microfluidic device. (a). A mixture of 10-105 µm MPs in pure water in 486 µm device when acoustic off and, (b). acoustic on. (c). A mixture of 10-20 µm and180-350 µm MPs suspended in pure water in the 1078-µm device when acoustic off and (d). Acoustic on. (e). A mixture of 180-212 µm MPs in 1% detergent and 1% fabric softener in the 1078-µm device when acoustic off and (f). Acoustic on. (g). A mixture of 10-20 µm and 180-212 µm MPs in 1% detergent and 1% softener medium in the 1078-µm device when acoustic off and (h). Acoustic on. Here, the large particles are focused on anti-nodes, and small particles are focused on nodes. The solid yellow lines indicate the boundaries of the microchannel, while broken yellow lines indicate the nodal planes.

According to equation 1, the primary acoustic radiation force is proportional to the cubed radius of the particle; hence, we can postulate that the focusing strength will be enhanced with the increase in particle size. The acoustic contrast factor will determine the transverse positioning of focused particles in the channel. According to equation (2), the contrast factor depends on MPs' density and compressibility relative to the medium. Therefore, we can expect MPs of the same material to focus on the same pressure nodal plane, regardless of their size, and larger MPs would be strongly focused. This trend of particle movement and focusing has been observed for most flow-through acoustic focusing applications reported so far, including the prior work on MP focusing by Akiyama Y et al [26]. However, particle sizes were significantly smaller than the wavelength in those studies, and the particle suspended medium was mainly water or an aqueous buffer. To the best of our knowledge, we report for the first time experimental studies on size-based two forms of focusing of particles of the same material in flow-through fluidic devices containing detergent and fabric softener in the medium. In this study, we observed small MPs, regardless of the change in the density of the aqueous medium, focused to the single pressure nodal plane of the 486 µm device, at a resonance frequency of 1.58 MHz, a minimum applied voltage of 6.2 V, and a maximum flow rate of 800 µL/min. Our flow rate is

relatively higher than what has been reported for MPs focusing [30]. However, even though we could utilize flow rates up to 1 mL/min at this applied voltage, the extent of focusing was not appreciated; thus, we limited all our microfluidic experiments to a maximum flow rate of 800 µL/min.

Condition	Focusing of Small MP	Focusing of Large MP	Frequency
Low density medium, Low frequency	Node	Node	710 KHz
Low density medium, High frequency	Node	Anti-node	1.38 MHz
High density medium, Low frequency	Node	Anti-node	710 KHz
High density medium, High frequency	Node	Anti-node	1.38 KHz

Table 1 A summary of MP focusing at different experimental conditions.

The focusing nature of MPs larger than 180 µm is different from smaller MPs at higher applied frequencies. Large MPs suspended in DI water, focused on the pressure node of the 1078-µm device, at a resonance frequency of 710 KHz, a minimum applied voltage of 3.8 V, and a maximum flow rate of 800 µL/min. However, these large particles focused to the anti-nodes of the 1078-µm device at a resonance frequency of 1.38 MHz. Also, these larger particles focused on the antinodal planes of the same device when the MPs were suspended in an aqueous medium containing 1% liquid detergent and 1% fabric softener, irrespective of the applied frequency. The measured density of the solution containing detergent and fabric softener was 1.18 g/mL. The experiment was repeated for smaller MP particles in 1% liquid detergent and 1% fabric softener to confirm that this observation was not device dependent. We observed that they focused on the pressure node of the 1078-µm device. To further confirm the observations,

we investigated focusing of a mixture of small and large MPs suspended in water and an aqueous medium containing 1% detergent and 1% fabric softener, respectively. All MPs suspended in water, regardless of the size, focused on the nodal plane of the device (see supplementary movie S1). However, the large MPs focused on the anti-nodes, and the small MPs focused on the nodal plane when they were suspended in softener and detergent containing medium (see supplementary movie S2). Our observations of MPs focusing on different conditions are summarized in Table 1. We did not observe any influence from particle concentration to the extent or the position of focusing, and it only depends on the size and the type of MPs. Though most MPs found in the environment are larger than 10 µm [35], this is the first time that acoustic focusing of MPs larger than 20 µm in diameter has been explored.

The antinodal focusing of large particles has been discussed theoretically before. However, any experimental observations have not yet been reported. Most work reported so far has utilized particles that are significantly smaller than the device equivalent wavelength. Hasegawa, T. has described that when the particle size is comparable to the wavelength, acoustic radiation force on particles can focus them to pressure antinodes at certain frequency ranges [36]. Hasegawa T. has shown the presence of alternative regions of antinodal focusing of larger particles. Habibi *et al.* have also recently discussed the same phenomenon, where they observed different particle focusing regimes with respect to the particle diameter normalized to the device wavelength (d/λ). Among them, when the d/λ is around 0.25-0.4 and 0.6-0.8, moderately rigid particles like PMMA and PS show antinodal focusing. They have shown that, with the increase of PMMA and PS particle size, the primary acoustic radiation force increases and remains positive until d/λ =0.25 in water. Hence, particles focus on the nodal planes. Around d/λ=0.25, primary acoustic radiative force (ARF) becomes negative and remains negative until d/λ reaches 0.425, this leads to the antinodal focusing of particles. Then the ARF become positive and stays positive until d/λ reaches 0.6, and becomes negative again [29]. In addition to the size

effects, the medium density also influences the antinodal focusing of particles in our system. The medium density changes when detergent and softener are present, which changes the acoustic contrast factor shown in equation (2). When the density of the medium increases, the value of the contrast factor becomes smaller; hence, these particles can easily obtain a negative contrast factor. As a result, particles with a diameter comparable to the wavelength of the applied frequency will focus on anti-nodes- for example, Olofsson. K. *et al.* recently demonstrated antinodal focusing of cells by changing the density of the medium [37]. Hence, it is clear that changes to medium density also play a vital role in antinodal focusing. In addition, we observed that large particles are formed into longitudinal chains during antinodal focusing (Fig. 2 f and h). The secondary acoustic forces are significant for large particles, a condition that differs from smaller particles. These secondary forces become dominant at antinodes, thus causing large particles to attract each other [29].

In the current study, when we used 300 µm particles in the single pressure node mode of 1078-µm device, the d/λ would be 0.14. At this condition, particles focused on the pressure node when they were suspended in water. When the medium density is greater than water and the applied frequency generates a single node, we observed these particles focused on anti-nodes. When the medium density is high, the acoustic contrast factor nears zero, causing particles to move to the anti-nodes before d/λ reaches 0.25. When the medium is water, and the applied frequency generates two nodes resulting in a d/λ value of 0.28, particles focus on the pressure anti-nodes (see supplementary figure S1). This observation can be confirmed by the theoretical study by Habibi *et al*. and Hasegawa. T. [29,36]. According to the best of our knowledge, this is the first instance to observe the combined effect of high density medium and d/λ effect to obtain antinodal focusing of particles. Acoustic focusing of small particles in viscus fluids is well studied. However, the effect of viscosity on acoustic focusing of large particles comparable to the wavelength has not been studied well. Since our study is based on 1% detergent in water,

we assumed the viscosity change to be negligible and it is a reasonable assumption between 23 ^{0}C-30 ^{0}C [38].

The medium density that MPs present in nature varies. The size of these MPs also varies. Hence, a system that can effectively remove MPs of any size and suspended in any medium has to be developed. When the density of the medium varies, the smaller and larger MPs focus on two different locations of the device. Therefore, a two-stage mechanism is envisioned and is discussed later in this section.

The minimum applied voltages required for focusing of three MP types at different flow rates were compared to understand the extent of MP focusing with respect to the type and size. When the acoustic focusing becomes weak, a higher applied voltage is required. As expected, all three MPs needed a higher applied voltage at high flow rates, as shown in Fig. 3. This was due to the shortened residence time, thus decreasing particle exposure to the acoustic field. Both PE and PMMA particles showed size-dependent voltage requirements; however, we did not observe a similar trend for PS particles, and all sizes required similar voltages. Overall, there was no significant variation of minimum voltage required based on the type of MP.

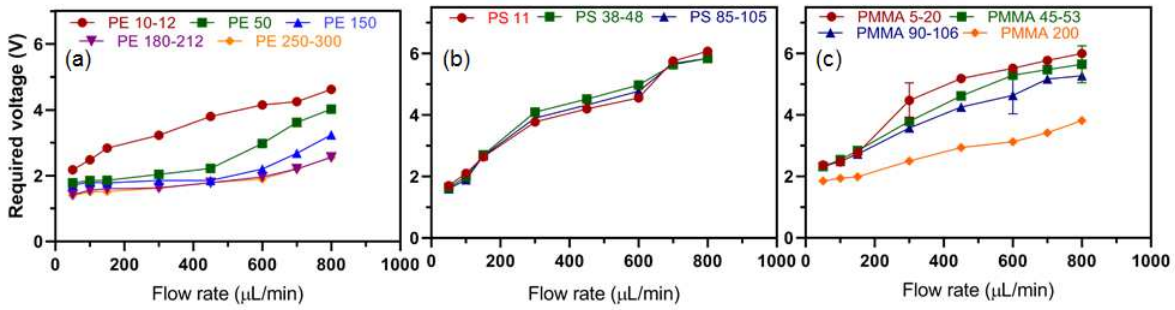

Fig. 3 The minimum voltage required for the effective focusing of three MP types at different flow rates. Particles larger than 150 µm were focused onto the antinodal planes of the device.

3.3 Determination of concentrating and focusing efficiencies

The concentrating and acoustic focusing efficiencies of MPs in a given device were determined to evaluate the device's performance. The concentrating efficiency will indicate how much MPs of the initial sample concentrated to a defined region of the device. The concentrating efficiencies at different flow rates were calculated by comparing the concentration (number of MPs particles per mL) of MPs in the device's central outlet at acoustic off and on conditions to the initial MPs concentration introduced to the device (equation 4). The focusing efficiency will indicate the distribution of the MPs in different regions of the device, thus enabling the accurate positioning of waste outlets. The focusing efficiency was determined by comparing the concentration of MPs in the middle stream to the total concentration of particles in the two outer streams as shown in equation (5), where C_m is the concentration of MPs exiting the middle stream and C_{lat} is the concentration of MPs exiting two lateral outlets. The performance of the microfabricated device was evaluated only for the MPs focusing on the nodal plane. Initially, the outlets of the microfluidic device used for MPs ⩾180 µm (1078-µm device) were designed to remove particles focusing on the two nodal planes of the device. However, in this study, we found that MPs ⩾ 180 µm are focused on the antinodal planes based on the medium density and d/λ, as mentioned earlier. Instead of designing a new microfluidic device to collect particles focused on pressure anti-nodes, we utilized the finding to create a suitable steel tube device that is more relevant for real applications.

$$Concentrating\ efficiency = \frac{Concentration\ of\ MPs\ in\ the\ central\ outlet}{Concentration\ of\ MPs\ in\ the\ initial\ sample} \quad (4)$$

$$Focusing\ efficiency = \left(\frac{C_m}{C_m + C_{lat}}\right) x100 \quad (5)$$

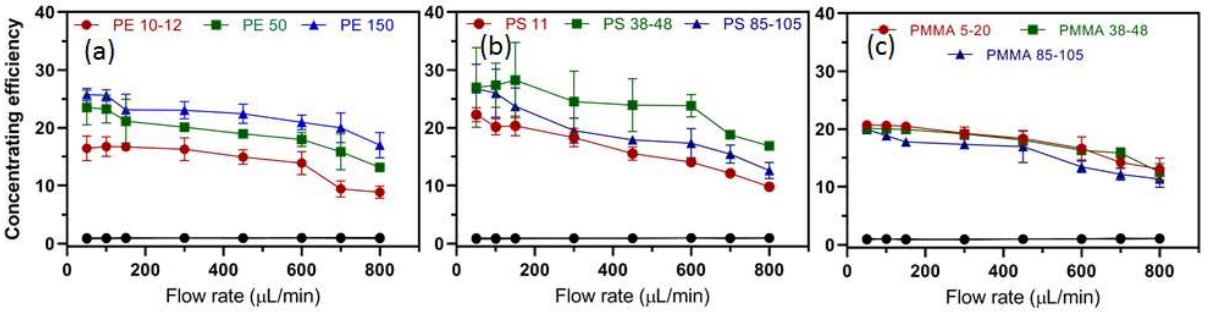

Fig. 4 Concentrating efficiencies of three MPs in the microfluidic device at different flow rates. (a). PE, (b). PS, and (c). PMMA. The trend lines for acoustic off conditions are shown in black.

Fig. 4 shows the concentrating efficiencies of three MPs types at varying flow rates. The black curves show that the concentrations of MPs exiting the device in the absence of acoustic forces were very similar to the initial concentrations, suggesting no observable sample loss during the process. In the presence of an applied acoustic field, MPs were concentrated by more than 16, 21, and 19 times for PE, PS, and PMMA, respectively, at 50 µL/min. When the flow rate increases, the concentration efficiency decreases as anticipated due to the short residence time thus, reducing exposure to the applied acoustic field. The concentration efficiencies were 8, 10, and 11 times for PE, PS, and PMMA, respectively, roughly a 50% reduction at a 16-fold flow rate increase.

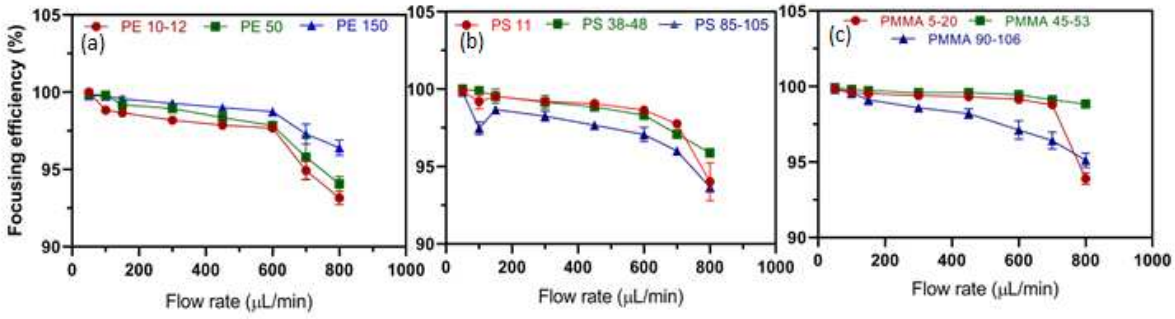

Fig. 5 Focusing efficiencies of three MPs at different flow rates (a) PE, (b) PS, (c) PMMA.

Fig. 5 shows no significant variation in focusing efficiencies for PE, PS, and PMMA MPs suggesting that particles were focused to the anticipated location of the device. Nevertheless, the focusing efficiency will be decreased by about 5% at flow rates greater than 600 µL/min. We limited the maximum applied voltage to 8 V during this study, and we anticipate that by increasing the applied voltage, we can accomplish a higher focusing efficiency.

As mentioned earlier, the data shown in Fig. 3, 4, and 5 were obtained using micro-fabricated devices with the width of 486 µm and 1078-µm to analyze small and large microplastics, respectively.

3.4 Removal of MPs using two-stage MP removal system

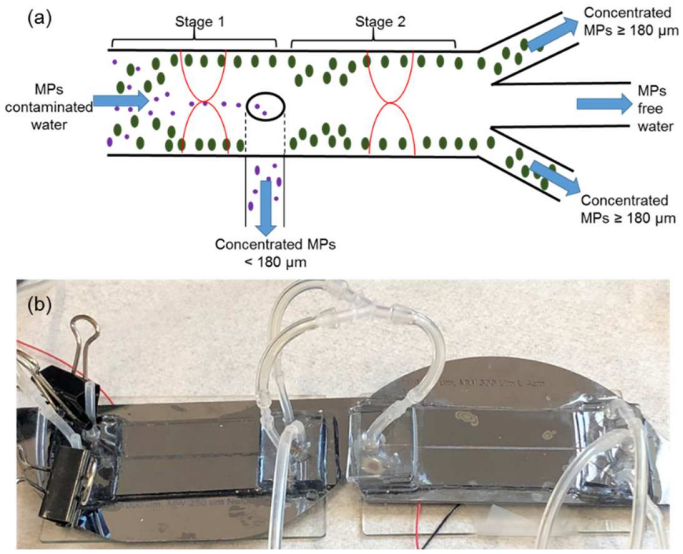

Fig. 6 (a). A schematic representation of an envisioned two-stage MPs removal system. MPs <180 µm are concentrated and isolated in the segment 1. Larger MPs are removed, and MPs-free water is collected via the middle outlet in the segment 2. (b). A two-stage MPs removal device. The two lateral outlets of the first device are connected to the inlet of the second device.

As shown in Fig. 6 (a), an acoustofluidic device with three outlets and two focusing segments can be designed to collect MPs concentrated on nodal and antinodal positions. In the first segment of the device, transducer 1 actuates at the resonance frequency, and the MPs focused on the center (pressure-node) are directed to a collection chamber. Likewise, in the second segment, particles focused to the two sides (pressure anti-nodes) will be directed to two lateral outlets, and the water free of MPs is collected via the middle outlet. This two-stage MPs removal system can be used for the effective removal of MPs in water samples with any density and for any MP type and size. As a proof of concept of using two-stage MP removal system to remove all the sizes of MPs suspended in any aqueous medium, two micro-fabricated devices with 1078 µm wide channels were connected in-line (Fig.6 b). Each device has a single inlet and three outlets and the two lateral outlets of the first device were connected to the inlet of the second device as shown in the Fig. 6 (b). A mixture of 300 µm (900 µg/mL) PE and 10-20 µm (300 µg/mL) PE suspended in 1% detergent and 1% fabric softener was introduced and 710 KHz at 6.2 V acoustic filed was applied to generate a single node in both devices. As discussed in Fig. 6 (a), the focused small MPs were collected from the middle outlet. The resulting MP free water was obtained from the middle outlet of the second device. Two lateral outlets of the second device were used to collect the concentrated large MPs. Equation (4) was used to compare the number of MPs left in samples collected from each outlet with the number of particles in the original sample. MPs were counted as described earlier in the methods section. We could collect 97.4% (± 0.5) of initial small MPs via the middle outlet of the first device, and 95.1% (± 1.6) of initial large MPs via two lateral outlets of the second device.

3.5 Acoustic focusing of microplastics in steel tube devices

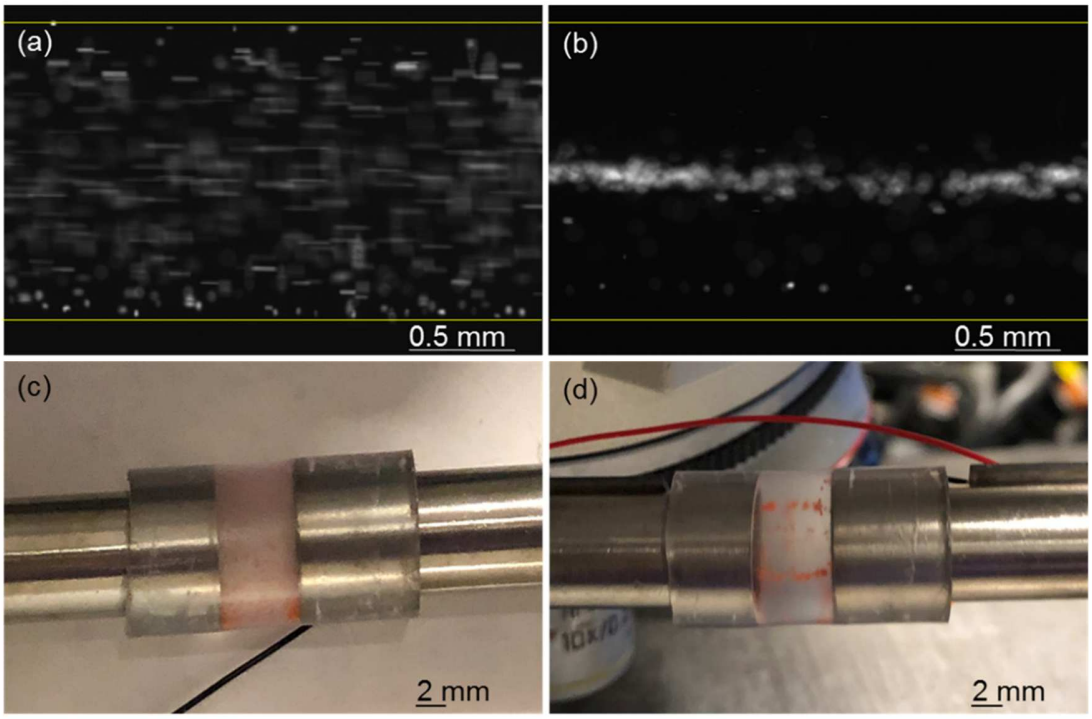

Fig. 7 (a). Acoustic focusing of MPs in steel tube devices. Fluorescence micrographs of a mixture of 5-50 µm PE, PS, and PMMA passing through an 1.4 mm I.D. steel tube in the absence, and (b). Presence of acoustic field. (c). Images of 180-212 µm PE suspended in 1% detergent and 1% softener, and particles passing through an 8 mm I.D. steel tube when acoustic off and (d). Acoustic on.

After key parameters of focusing were characterized using microfabricated devices, acoustic focusing of MPs was explored in larger devices constructed using readily available, inexpensive steel tubes that can facilitate higher flow rates (Fig. 7, supplementary Movies S3 and S4). The resonance frequency (v) for *n* number of pressure nodes can be predicted from the equation (6)[32], where U is the sound velocity in the medium and l is the diameter of the tube. The number of anti-nodes at v is *n+1*.

$$v = \frac{U\,n}{2\,l} \qquad (6)$$

Fig. 7 (a) and (b) show the movement of a mixture of small MPs (5-50 µm) in the absence and presence of an acoustic field, respectively. As in microfluidic experiments, small microplastics focused on the pressure node of the steel device regardless of the suspended medium or the wavelength of the applied frequency. Here, we used 1.4 mm ID steel tube to demonstrate the focusing. We used the 10X objective of the epifluorescence microscope for visualization purposes as the particles were too small to see through the naked eye. Here, we used a device small enough to capture fluorescence images of the entire device via an epi-fluorescence microscope. A single pressure node is generated at a resonance frequency of 556 KHz. Next, we tested acoustic focusing of larger MPs (PE 180-212 µm) suspended in 1% detergent and 1% softener medium in the absence (Fig. 7 c) or presence (Fig. 7 d) of an acoustic field. Standing acoustic waves with a resonance frequency of 290 KHz were applied to generate four pressure anti-nodes in an 8 mm I.D. steel tube. Two of the four focused streams are in different depths of field of view in the images captured with a cell phone (Fig. 7 d). From the applications' perspective, it is convenient to have a minimum number of concentrated streams (thus, a minimum number of tubing at the outlet); therefore, the number of focused streams generated was restricted to the minimum by keeping the frequency low. We could try to generate two pressure anti-nodes at a resonance frequency lower than 290 KHz, however; the strength of the acoustic forces diminishes with the decrease in frequency. It is clear from Fig. 7 b that a small portion of particles was not effectively focused to the two streams, and this was also evident from our concentrating efficiency measurements, as shown in Fig. 8.

The concentration efficiency was determined using a steel tube with branched outlets. The placement of the outlets was dictated by the particle size, wavelength of the applied frequency, and the medium density. The top left panel in Fig. 8 shows the cross-section of the outlet employed to collect smaller MPs, where circle 1 depicts a larger tubing placed at the core of

the metal tube to collect smaller MPs concentrated at the center while circles 2-7 represent smaller tubing located laterally. The branched outlet with eight tubings (numbered 1-8) shown in the top right panel in Fig. 8 was employed to collect larger MPs. The concentration and focusing efficiencies were calculated using equations (3) and (4), respectively. In steel tubes, C_m for MPs < 180 µm was the concentration of MPs coming out of outlet 1, while C_{lat} was the sum of the concentrations of particles from outlets, two through seven (Fig. 8, top left). For MPs >180 µm, the C_m was the sum of the concentrations of particles from outlets 1,2,3, and 4 and $C_{lat}$was the sum of the concentrations of particles from outlets 5,6,7, and 8 as shown in Fig. 8 top right panel.

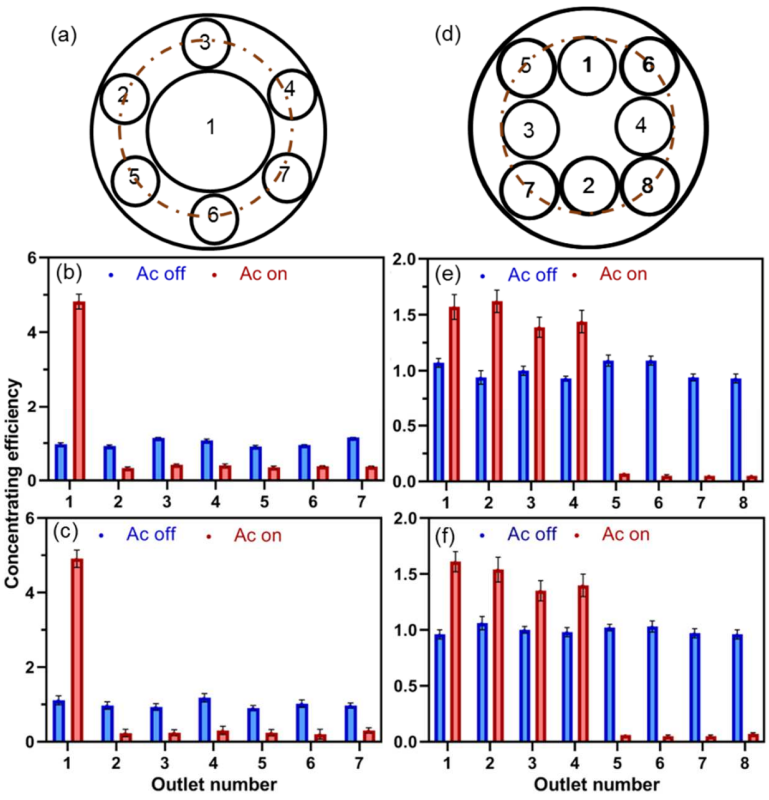

Fig. 8 Concentrating efficiencies for four sizes of PE MPs in 8 mm ID steel tube devices operating at 290 KHz, 2.3 V, and 12 mL/min. The outer large black circle represents the steel tube and the inner small black circles represent the position of the outlets located at the end of

the second steel tube of the steel device. The dashed lines indicate the concentric patterning of outlets. Concentration of MPs coming out of each labelled outlet is shown in the graphs. (a). 10-12 µm, (b). 50 µm, (c). 180 -212 µm, and (d). 250-300 µm.

We did not integrate the two separating segments together for the proof of the concept study and quantification described here. Instead, the two stages were analyzed separately using MPs suspended in aqueous media containing 1% detergent and 1% softener. Our concentrating efficiency data suggest that small PE particles were uniformly distributed among 7 outlets in the absence of an acoustic field (blue bars in Fig. 8 a & b), and they were concentrated to the middle outlet by five-fold in the presence of the acoustic field. Thus, 70% (+/-3) of the initial small MPs were concentrated in the middle outlet. Large MPs were also evenly distributed among eight outlets before applying the acoustic field and then concentrated six-fold to the four lateral outlets when the acoustic field was on. This is about 82% (+/-5) of the initial MPs. From a practical perspective, the amount of removal must be improved. We anticipate that applying higher voltage, optimizing the outlet's placement, using a transducer that is optimized to the resonance frequency of the tube, and using an extended transducer will improve the concentrating and focusing efficiency significantly, thus an increase in MPs removal. In addition, employing acoustic transducers optimized for resonance frequencies will significantly enhance the focusing strength. Having a plastic connector as the optical window can also decrease the removal efficiency. If an optical window is needed, we can customize the device with a glass connector.

4. Conclusions

In the present study, we have demonstrated the acoustic focusing of MPs of PS, PMMA, and PE with sizes ranging from 6 µm to 300 µm in diameter, first with devices constructed with silicon microchannel and then millimeter-scale steel tubes. We have shown that acoustic

focusing of MPs with a size comparable to the resonance acoustic wavelength is influenced by both the medium density and the acoustic frequency. Hence, MPs of the same material can have two different focusing patterns for different sizes. We demonstrated that larger MP particles would focus on pressure antinodes instead of nodes at high acoustic frequency, regardless of the medium density. On the other hand, if both frequency and the medium density are low, particles will focus on the pressure node, regardless of the size. Microfluidic devices are not compatible with most real application settings, however, our approach with steel tubes can be further modified and expanded for high flow rate, and large volume systems. Though we had only 70% extraction of smaller microplastics and 82% larger microplastics at 12 mL/min in our short steel acoustic device, we anticipate by having a longer steel tube with continuous acoustic actuation, and acoustic transducers optimized for the resonance frequency will provide a much better focusing efficiency, hence an enhanced particle extraction. Further, we envision that having a large pipe branched into smaller acoustically resonating pipes can provide a flow-through, filter-free method to isolate microplastics effectively and efficiently without clogging issues. Our approach can also be used to concentrate microplastics of varying sizes for detection and chemical analysis. Our future studies include the investigation of MPs with different shapes and influences from other water sources, including seawater.

Declaration of competing interest The authors declare that they have no known competing financial interests or personal relationships that could have appeared to influence the work reported in this paper.

Acknowledgement This work was performed, in part, at the Center for Integrated Nanotechnologies, an Office of Science User Facility operated for the U.S. Department of Energy (DOE) Office of Science by Los Alamos National Laboratory (Contract DE-AC52-06NA25396) and Sandia National Laboratories (Contract DEAC04-94AL85000).

References

[1] C.G. Avio, S. Gorbi, F. Regoli, Plastics and microplastics in the oceans: From emerging pollutants to emerged threat, Marine Environmental Research, 128(2017) 2-11.
[2] S. Lambert, M. Wagner, Microplastics are contaminants of emerging concern in freshwater environments: an overview, Freshwater microplastics, Springer, Cham2018, pp. 1-23.
[3] R.C. Thompson, Y. Olsen, R.P. Mitchell, A. Davis, S.J. Rowland, A.W. John, et al., Lost at sea: where is all the plastic?, Science, 304(2004) 838-.
[4] A.B. Silva, A.S. Bastos, C.I.L. Justino, J.P. da Costa, A.C. Duarte, T.A.P. Rocha-Santos, Microplastics in the environment: Challenges in analytical chemistry - A review, Analytica Chimica Acta, 1017(2018) 1-19.
[5] A. van Wezel, I. Caris, S.A.E. Kools, Release of primary microplastics from consumer products to wastewater in the Netherlands, Environmental Toxicology and Chemistry, 35(2016) 1627-31.
[6] R.M. Blair, S. Waldron, V. Phoenix, C. Gauchotte-Lindsay, Micro- and Nanoplastic Pollution of Freshwater and Wastewater Treatment Systems, Springer Science Reviews, 5(2017) 19-30.
[7] M. Bergmann, V. Wirzberger, T. Krumpen, C. Lorenz, S. Primpke, M.B. Tekman, et al., High Quantities of Microplastic in Arctic Deep-Sea Sediments from the HAUSGARTEN Observatory, Environmental Science & Technology, 51(2017) 11000-10.
[8] M.A. Browne, P. Crump, S.J. Niven, E. Teuten, A. Tonkin, T. Galloway, et al., Accumulation of Microplastic on Shorelines Woldwide: Sources and Sinks, Environmental Science & Technology, 45(2011) 9175-9.
[9] M.A. Browne, T.S. Galloway, R.C. Thompson, Spatial Patterns of Plastic Debris along Estuarine Shorelines, Environmental Science & Technology, 44(2010) 3404-9.
[10] M. González-Pleiter, M. Tamayo-Belda, G. Pulido-Reyes, G. Amariei, F. Leganés, R. Rosal, et al., Secondary nanoplastics released from a biodegradable microplastic severely impact freshwater environments, Environmental Science: Nano, 6(2019) 1382-92.
[11] J. Haap, E. Classen, J. Beringer, S. Mecheels, J.S. Gutmann, Microplastic Fibers Released by Textile Laundry: A New Analytical Approach for the Determination of Fibers in Effluents, Water, 11(2019) 2088.
[12] I.E. Napper, R.C. Thompson, Release of synthetic microplastic plastic fibres from domestic washing machines: Effects of fabric type and washing conditions, Marine Pollution Bulletin, 112(2016) 39-45.
[13] R. Geyer, J. Jambeck, K. Law, Production, use, and fate of all plastics ever made, Science advances, 3(2017) e1700782-e.
[14] S.-J. Royer, S. Ferrón, S.T. Wilson, D.M. Karl, Production of methane and ethylene from plastic in the environment, PLOS ONE, 13(2018) e0200574.
[15] S.L. Wright, F.J. Kelly, Plastic and human health: a micro issue?, Environmental science & technology, 51(2017) 6634-47.
[16] C.M. Boerger, G.L. Lattin, S.L. Moore, C.J. Moore, Plastic ingestion by planktivorous fishes in the North Pacific Central Gyre, Marine Pollution Bulletin, 60(2010) 2275-8.
[17] C.G. Avio, S. Gorbi, F. Regoli, Experimental development of a new protocol for extraction and characterization of microplastics in fish tissues: First observations in commercial species from Adriatic Sea, Marine Environmental Research, 111(2015) 18-26.
[18] M. Cole, P. Lindeque, E. Fileman, C. Halsband, R. Goodhead, J. Moger, et al., Microplastic Ingestion by Zooplankton, Environmental Science & Technology, 47(2013) 6646-55.
[19] Y. Wang, D. Zhang, M. Zhang, J. Mu, G. Ding, Z. Mao, et al., Effects of ingested polystyrene microplastics on brine shrimp, Artemia parthenogenetica, Environmental Pollution, 244(2019) 715-22.

[20] L.G.A. Barboza, A. Dick Vethaak, B.R.B.O. Lavorante, A.-K. Lundebye, L. Guilhermino, Marine microplastic debris: An emerging issue for food security, food safety and human health, Marine Pollution Bulletin, 133(2018) 336-48.
[21] K.D. Cox, G.A. Covernton, H.L. Davies, J.F. Dower, F. Juanes, S.E. Dudas, Human Consumption of Microplastics, Environmental Science & Technology, 53(2019) 7068-74.
[22] J. Talvitie, A. Mikola, A. Koistinen, O. Setälä, Solutions to microplastic pollution – Removal of microplastics from wastewater effluent with advanced wastewater treatment technologies, Water Research, 123(2017) 401-7.
[23] M. Claessens, L. Van Cauwenberghe, M.B. Vandegehuchte, C.R. Janssen, New techniques for the detection of microplastics in sediments and field collected organisms, Marine Pollution Bulletin, 70(2013) 227-33.
[24] R. Rodríguez-Alegre, J.E. Sánchez-Ramírez, L. Pastor, S. Doñate, A. Marí, A. Lara, et al., Microplastics Extraction and Counting from Wastewater and Sludge Through Elutriation and Hydrocyclone, Springer International Publishing, Cham, 2020, pp. 53-9.
[25] C.K. Chen, J. Zhang, A. Bhingarde, T. Matotek, J. Barrett, B.D. Hardesty, et al., A portable purification system for the rapid removal of microplastics from environmental samples, Chemical Engineering Journal, 428(2022) 132614.
[26] M.E. Piyasena, P.P. Austin Suthanthiraraj, R.W. Applegate Jr, A.M. Goumas, T.A. Woods, G.P. López, et al., Multinode acoustic focusing for parallel flow cytometry, Analytical chemistry, 84(2012) 1831-9.
[27] G.T. Silva, Acoustic radiation force and torque on an absorbing compressible particle in an inviscid fluid, The Journal of the Acoustical Society of America, 136(2014) 2405-13.
[28] G.T. Silva, H. Bruus, Acoustic interaction forces between small particles in an ideal fluid, Physical Review E, 90(2014) 063007.
[29] R. Habibi, C. Devendran, A. Neild, Trapping and patterning of large particles and cells in a 1D ultrasonic standing wave, Lab on a Chip, 17(2017) 3279-90.
[30] Y. Akiyama, T. Egawa, K. Koyano, H. Moriwaki, Acoustic focusing of microplastics in microchannels: A promising continuous collection approach, Sensors and Actuators B: Chemical, 304(2020) 127328.
[31] G.P. Gautam, T. Burger, A. Wilcox, M.J. Cumbo, S.W. Graves, M.E. Piyasena, Simple and inexpensive micromachined aluminum microfluidic devices for acoustic focusing of particles and cells, Analytical and Bioanalytical Chemistry, 410(2018) 3385-94.
[32] P.P.A. Suthanthiraraj, M.E. Piyasena, T.A. Woods, M.A. Naivar, G.P. López, S.W. Graves, One-dimensional acoustic standing waves in rectangular channels for flow cytometry, Methods, 57(2012) 259-71.
[33] W.P. de Haan, A. Sanchez-Vidal, M. Canals, N.S.S. Party, Floating microplastics and aggregate formation in the Western Mediterranean Sea, Marine pollution bulletin, 140(2019) 523-35.
[34] B.C. Colson, A.P.M. Michel, Flow-Through Quantification of Microplastics Using Impedance Spectroscopy, ACS Sensors, (2021).
[35] V. Hidalgo-Ruz, L. Gutow, R.C. Thompson, M. Thiel, Microplastics in the Marine Environment: A Review of the Methods Used for Identification and Quantification, Environmental Science & Technology, 46(2012) 3060-75.
[36] T. Hasegawa, Acoustic radiation force on a sphere in a quasistationary wave field—theory, The Journal of the Acoustical Society of America, 65(1979) 32-40.
[37] K. Olofsson, B. Hammarström, M. Wiklund, Acoustic separation of living and dead cells using high density medium, Lab on a chip, 20(2020) 1981-90.
[38] L.M. Kushner, W.D. Hubbard, R.A. Parker, Turbidity and viscosity measurements on some cationic detergents in water and in sodium chloride solutions, Journal of Research of the National Bureau of Standards, 59(1957).

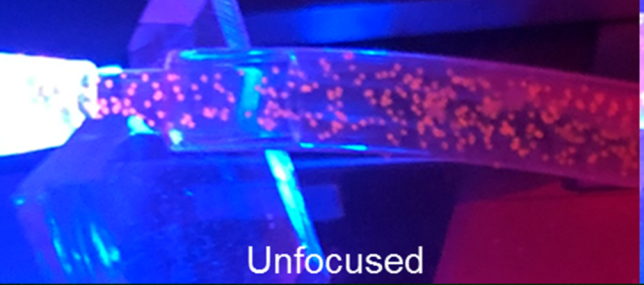
Unfocused

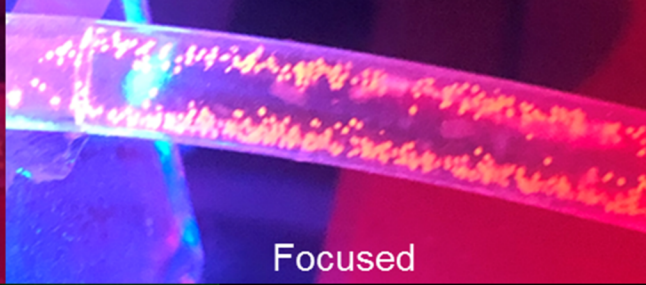
Focused

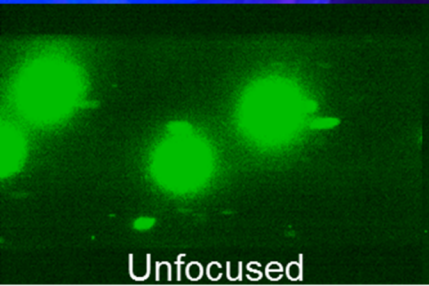
Unfocused

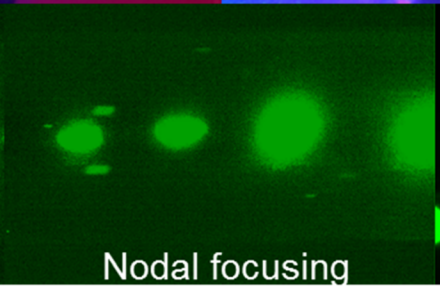
Nodal focusing

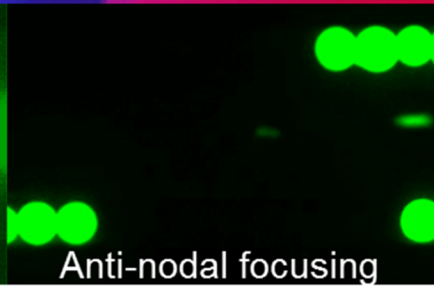
Anti-nodal focusing